Supplementary Information

Molecularly-induced roughness and oxidation in cobalt/organodithiol/cobalt nanolayers synthesized by sputter-deposition and molecular sublimation, Rowe, Shanmugam, Greczynski, Hultman, le Febvrier, Eklund, Ramanath

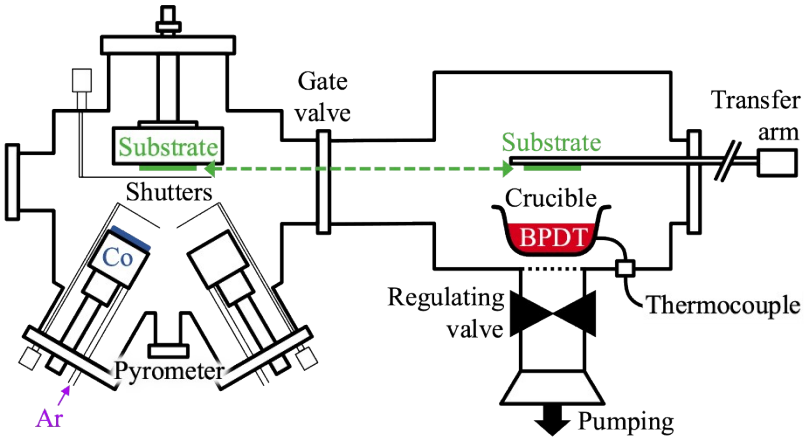

Fig. S1. Schematic of the ultra-high vacuum chamber used for metal sputter-deposition[1] with attached load-lock chamber containing a crucible for subliming BPDT flux for MNL formation. The schematic is not to scale.

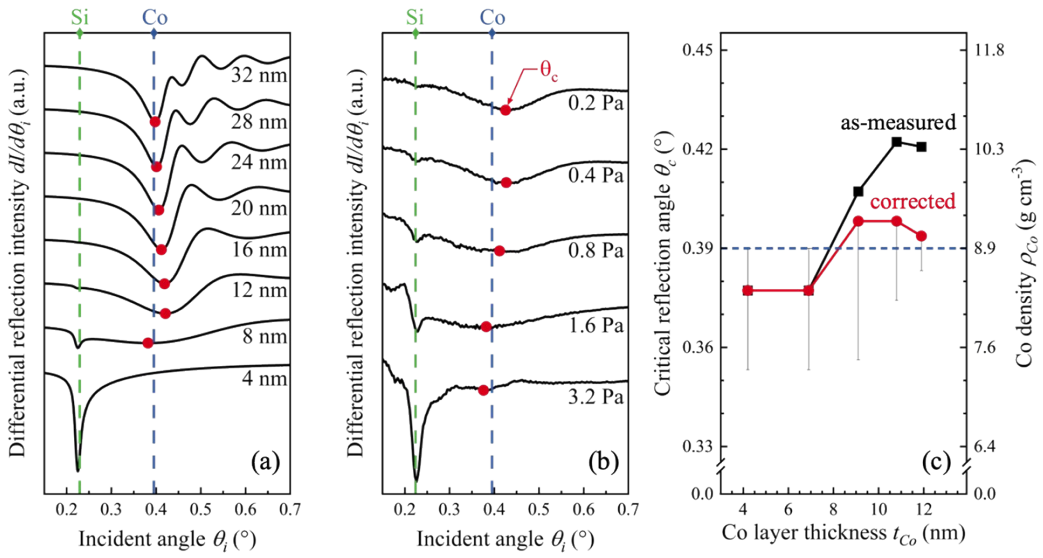

Fig. S2. (a) Differential XRR intensity from the first Co layer deposited on Si at different p_{Ar}. Red points indicate the $dI/d\theta$ minima corresponding to θ_c for Co. (b) Representative simulations assuming a constant ρ_{Co} showing θ_c shifts with t_{Co} due to Kiessig interference. Dashed vertical lines indicate θ_c for bulk Co and Si. (c) As-measured θ_c (squares) and corrected θ_c (circles) and associated ρ_{Co} plotted versus t_{Co}. The horizontal dashed line denotes ρ_{Co} and θ_c for bulk Co.

XRR data fits with Kiessig fringes simulations of model Co/SiO_2/Si structures were insensitive to ρ_{Co}. We thus determined ρ_{Co} from the total external reflection angle[2-4] θ_c identified by the $dI/d\theta$ minimum for the Co layer. Down shifts in θ_c with decreasing t_{Co} are expected because the Co layer thicknesses ($4 \leq t_{Co} \leq 12$ nm) on the lower refractive index SiO_2/Si substrate are comparable to the X-ray attenuation depth $d_{1/e} \sim 6.6$ nm for bulk Co at θ_c. The θ_c up-shifts (Fig. S2a) are due to t_{Co}-dependent low-order Kiessig fringe interference with the $dI/d\theta$ minimum. XRR intensity simulations for Co layers with *constant* bulk densities but different thicknesses t_{Co} show θ_c up-shifts (Fig. S2b) which incorrectly imply that ρ_{Co} relates to t_{Co}. To correct for this Kiessig interference-induced θ_c up-shift artifact, we determined the difference between the simulated θ_c values for a constant bulk density, and θ_c calculated from $\rho_{Co} = \frac{\theta_c^2 \pi M_A}{N_A r_e \lambda^2 f_1}$ (M_A = atomic mass, N_A = Avogadro number, r_e = classical electron radius, λ = X-ray wavelength, and f_1 = real part of the

atomic scattering factor). This correction was then applied to measured θ_c and plotted as a function of t_{Co} determined from Kiessig fringe simulations which are insensitive to ρ_{Co} (Fig. S2c).

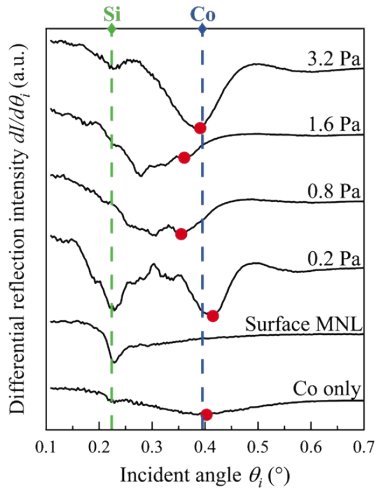

Fig. S3. Differential XRR intensity from Co/BPDT MNL/Co sandwiches with the top Co layer deposited at different p_{Ar}. The red points show the calculated θ_c by $dI/\mathrm{d}\theta$ minima in the region expected for Co.

We determined θ_c using $dI/d\theta$ minima in differential XRR intensity characteristics from Co/BPDT MNL/Co sandwiches (Fig. S3). However, simulations from idealized layers Co/MNL/Co model structures were inadequate to capture the features of the measured data due to several factors such as surface Co oxidation and roughening (Fig. 6).

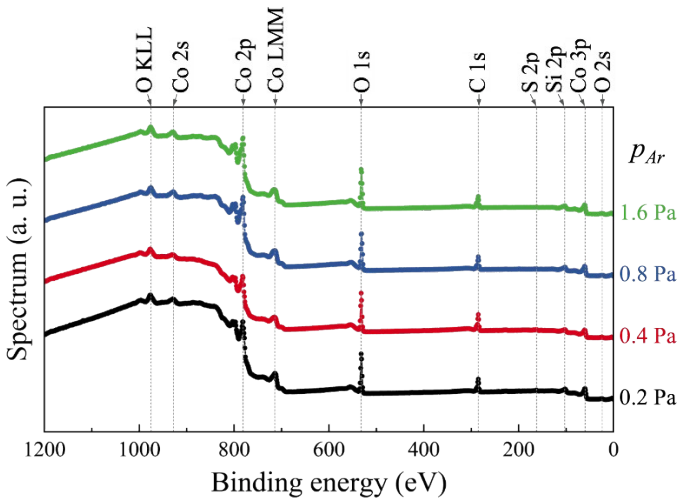

Fig. S4. Representative XPS survey spectra for variable p_{Ar} with the most prominent peaks labeled. Measurements were collected with the surface-to-detector angle θ_{SD} = 30°.

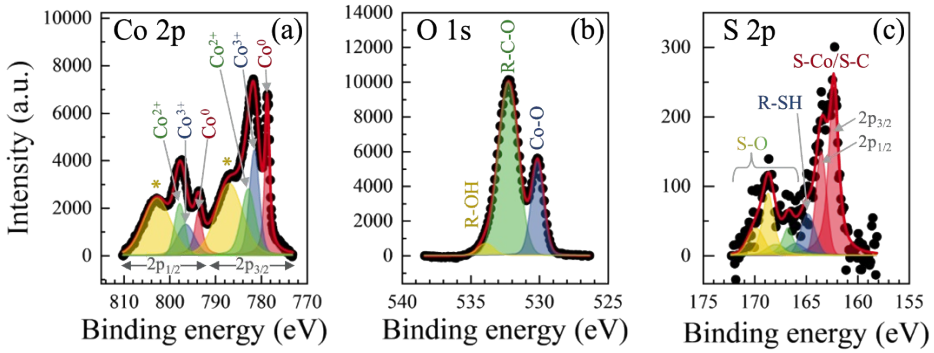

Fig. S5. Example XPS spectra in the vicinity of the (a) Co 2p, (b) O 1s and (c) S 2p bands, shown along with the detailed sub-band peak fits used to identify the chemical states. The $2p_{3/2}$ and $2p_{1/2}$ sub-bands associated with Co and S chemical states are shown where applicable. "*" denotes the Co satellite peak.

Supplementary References

1. A. le Febvrier, L. Landälv, T. Liersch, D. Sandmark, P. Sandström, P. Eklund, *Vacuum*, 2021, **187**, 110137.
2. L. G. Parratt, *Physical Review*, 1954, **95**, 359-369.
3. M. Saito, S. Sato, Y. Waseda, *High Temperature Materials and Processes*, 1998, **17**, 117-132.
4. B. L. Henke, E. M. Gullikson, J. C. Davis, *Atomic Data and Nuclear Data Tables*, 1993, **54**, 181-342.